

# Arrhythmia Discrimination in Implantable Cardioverter Defibrillators Using Support Vector Machines Applied to a New Representation of Electrograms

Paola Milpied\*, Rémi Dubois, *Member, IEEE*, Pierre Roussel, Christine Henry, and Gérard Dreyfus, *Senior Member, IEEE*

**Abstract**—Arrhythmia classification remains a major challenge for appropriate therapy delivery in implantable cardioverter defibrillators (ICDs). The purpose of this paper is to present a new algorithm for arrhythmia discrimination based on a statistical classification by support vector machines of a novel 2-D representation of electrograms (EGMs) named spatial projection of tachycardia (SPOT) EGMs. SPOT-based discrimination algorithm provided sensitivity and specificity of 98.8% and 91.3%, respectively, on a test database. A simplified version of the algorithm is also presented, which can be directly implemented in the ICD.

**Index Terms**—Arrhythmias, electrogram (EGM) morphology, implantable cardioverter defibrillators (ICDs), inappropriate therapy, spatial projection of tachycardia (SPOT), support vector machines (SVMs).

## I. INTRODUCTION

UNLIKE supraventricular tachycardia (SVT), ventricular tachycardia (VT) is a life-threatening tachyarrhythmia that may lead to sudden death unless an appropriate shock is delivered. It aims at resynchronizing cardiac cells to restore a normal rhythm. Unfortunately, inappropriate shocks are very painful and stressful for patients, and can also trigger a life-threatening tachyarrhythmia. Therefore, discrimination of VT from SVT is a major challenge for appropriate therapy delivery in implantable cardioverter defibrillators (ICDs). In a dual-chamber device, two leads are implanted, one in the right atrium and one in the right ventricle, with a decision based on both signals. For primary prevention, however, a single-chamber device is usually

Manuscript received July 23, 2010; revised January 7, 2011; accepted February 1, 2011. Date of publication February 22, 2011; date of current version May 18, 2011. This work was supported in part by Sorin CRM and in part by the French National Association for Technical Research (ANRT). *Asterisk indicates corresponding author.*

\*P. Milpied is with the Department of Advanced Clinical Research, Sorin CRM, 92143 Clamart, France, and also with the Signal Processing and Machine Learning (SIGMA) Laboratory, École Supérieure de Physique et de Chimie Industrielles (ESPCI) ParisTech, 75231 Paris, France (e-mail: paola.milpied@sorin.com).

R. Dubois, P. Roussel, and G. Dreyfus are with the Signal and Machine Learning (SIGMA) Laboratory, École Supérieure de Physique et de Chimie Industrielles (ESPCI) ParisTech, 75231 Paris, France (e-mail: remi.dubois@espci.fr; pierre.roussel@espci.fr; gerard.dreyfus@espci.fr).

C. Henry is with the Department of Advanced Clinical Research, Sorin CRM, 92143 Clamart, France (e-mail: christine.henry@sorin.com).

Digital Object Identifier 10.1109/TBME.2011.2117424

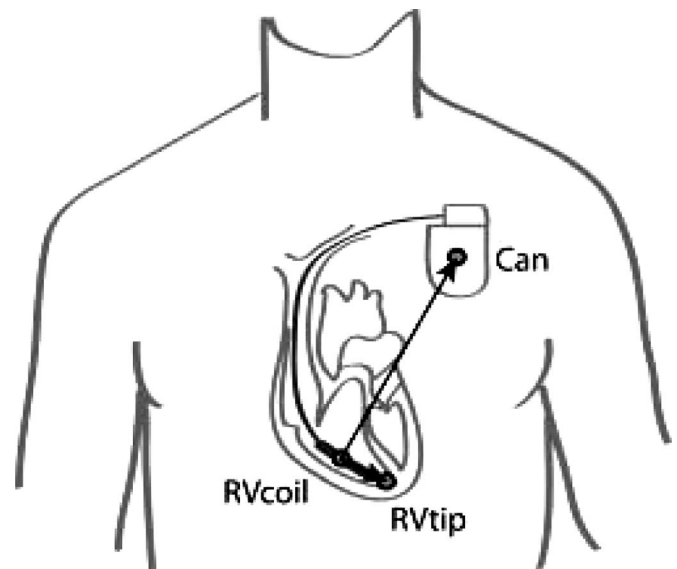


Fig. 1. Simplest ICD system: a single-chamber ICD with a single-coil integrated bipolar lead. The distal electrode (tip) has a small area and is located in the apex (or the septum) of the right ventricle (RV). The proximal electrode (coil) is an elongated electrode located in the RV, close to the tip; this electrode delivers the electrical shock if necessary, together with the can as the reference; the latter is generally implanted in left subclavicular position.

preferred. In such devices, a single lead is implanted in the right ventricle and arrhythmia discrimination is based on information pertaining solely to the ventricles.

The Madit II study [1] was the first to document the life-saving benefits of single- and dual-chamber ICDs in a primary prevention population with long-term data. The results of the study showed that inappropriate shocks occurred commonly: 11.5% of the 719 ICD patients were shocked inappropriately, and the number of inappropriate shocks represented 31.2% of the total number of shock episodes. Besides the pain and stress inflicted by inappropriate shocks to the patient, Madit II also showed that they were associated with increased risk of all-cause mortality. There is thus clearly a need for further improvements in arrhythmia discrimination.

The discrimination in ICDs is performed from endocardial measurements of the electrical activity of the heart between electrodes called electrograms (EGMs) (see Fig. 1). Historically, only time intervals extracted from EGMs were used

for diagnosis. In the last decade, however, when ICDs began to be equipped with sufficient computing power, an analysis of the shape of a single EGM channel was added, resulting in improved performances [2]–[4]. Nevertheless, no consensus has emerged on the choice of the most appropriate channel for best performance. Boriani *et al.* [5], for example, performed their morphology algorithm on bipolar intraventricular EGMs (RVcoil-RVtip). Conversely, Luthje *et al.* [6] and Wolber *et al.* [7] showed that RVcoil-can EGM appears to be superior to other EGM sources. Finally, Gold *et al.* [3] used a “dual-coil lead,” a special lead with an additional defibrillation coil, in order to provide a more global view of electrical conduction throughout the heart. In this paper, we propose to perform a morphological analysis from both far-field (RVcoil-can) and near-field (RVcoil-RVtip) EGMs recorded using any standard lead. The main contribution of this paper is the description of these two EGMs in an appropriate 2-D space in which the discrimination of the arrhythmia can be efficiently performed.

This new representation, termed spatial projection of tachycardia (SPOT), together with the mathematical features for its description, are presented in Section II. Section III provides an overview of the discrimination algorithm based on SPOT representation and introduces the statistical classifier developed in this study. Section IV presents the performances of the proposed method, while complexity considerations for hardware implementation are discussed in Section V. Section VI concludes the paper.

## II. SPATIAL PROJECTION OF TACHYCARDIA

### A. Physiological Basis and EGM Signals

It is known from physiological knowledge on cardiac arrhythmia that electrical propagation on the cardiac muscle pertaining to both normal heartbeats and SVT originates in the atria. Consequently, the conduction pathways followed in the ventricles are also the same. Conversely, the VT electrical signal, which originates in the ventricles themselves, uses a different pathway. This property results in morphological differences between normal and VT beat EGMs, while normal and SVT beat EGMs are rather similar.

Consequently, the proposed SVT versus VT discrimination method relies essentially on the differences in shape between arrhythmic EGM signals and normal beat signals. In addition, when analyzing a body surface ECG, it is commonly accepted that a single ECG channel is not enough to precisely understand the underlying activity of the heart. Indeed, an ECG is a 1-D projection of the electrical activity along the direction spanned by the electrodes, and 2, 3, or 12 leads are usually preferred. This property can be generalized to EGM signals. Thus, the study aims at simultaneously analyzing two EGMs, which are available at the same time: the far-field and the near-field signals.

### B. SPOT Curve Representation

The two EGM channels that record the ventricular depolarization are plotted in a 2-D space in which the  $x$ -axis is the voltage amplitude of the far-field signal and the  $y$ -axis the voltage am-

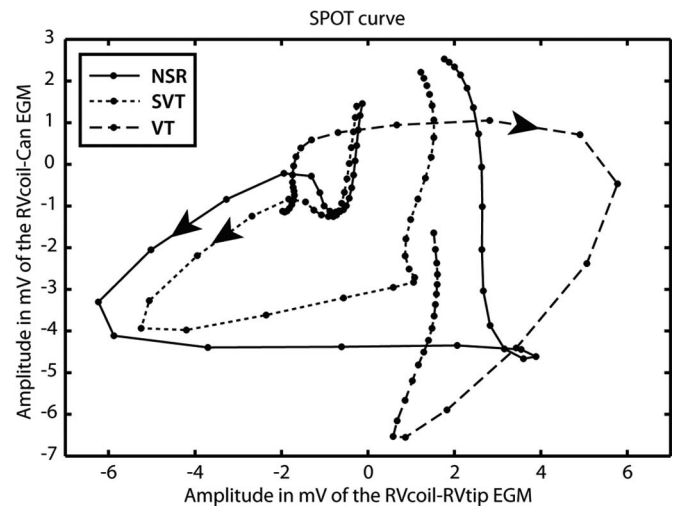


Fig. 2. Three SPOT curves for a single patient. For illustration, EGMs are sampled at 500 Hz.

plitude of the near-field signal in the spirit of vectocardiograms used in the analysis of surface ECGs. Thus, this plot provides a compact representation of two different physical signals, carrying different information; this is a sharp contradistinction to state-space plots that represent the time evolution of a single signal [8]. In our representation, called SPOT, a cardiac cycle is represented by a loop, with time as a parameter. Fig. 2 shows three SPOT curves for the same patient, one during a normal sinus rhythm (NSR), one during a VT, and one during an SVT. As expected, the SVT SPOT curve is similar to the NSR SPOT curve up to a scale factor that will be discussed in the following, while the VT SPOT curve is very different in both direction and shape.

### C. Description of a Single SPOT Curve

As we wish to make comparisons among SPOT curves, relevant numerical descriptors are required for these curves. The choice of these has been driven by physiological observations and statistical feature selection, and results in the selection of the velocity vector as a good quantitative value [9].

Let  $b(t)$  be the amplitude of the bipolar near-field signal, and  $u(t)$  the amplitude of the unipolar far-field signal at time  $t$ . Velocity vectors are computed as the time derivatives of each EGM channel. We denote by  $u'(t)$  and  $b'(t)$  the time derivatives of  $u(t)$  and  $b(t)$ , respectively, by  $\mathbf{V}(t) = (b'(t), u'(t))$  the velocity vector at time  $t$ , and by  $N(t)$  the Euclidean norm of  $\mathbf{V}(t)$ .

### D. Comparison Between Two SPOT Curves

Three elements of prior physiological knowledge served as guidelines in the selection of relevant features for the discrimination between SPOT curves.

First, the electrodes are essentially motionless inside the heart. In other words, electrical activities along similar conduction pathways should result in consistently similar directions of the velocity vectors along the SPOT curves (this property will be called “directional consistency”).

TABLE I  
FEATURE COMPUTATION

Arrhythmia SPOT curve tested	$\langle\theta\rangle$	$C$
VT	1.3 rad = 76°	0.70
SVT	0.3 rad = 18°	0.94

Second, the velocity of the depolarization wave should vary in the same way for NSR and SVT SPOT curves (this property will be called “velocity consistency”).

Finally, the amplitude of the signals may vary; thus, two homothetic SPOT curves should not be considered as different: the selected features should comply with this constraint.

In order to evaluate directional consistency quantitatively, the candidate feature is the average value  $\langle\theta\rangle$  of the angles between relative velocity vectors  $\mathbf{V}(t)$  from the two SPOTs to be compared. Let  $\theta(t)$  be this angle at time  $t$

$$\cos(\theta(t)) = \frac{\mathbf{V}_1(t) \cdot \mathbf{V}_2(t)}{N_1(t)N_2(t)} = \frac{b'_1(t)b'_2(t) + u'_1(t)u'_2(t)}{N_1(t)N_2(t)} \quad (1)$$

where  $\mathbf{V}_1(t)$  and  $\mathbf{V}_2(t)$  are the velocity vectors at time  $t$  associated to the two SPOTs to be compared, and  $N_1(t)$  and  $N_2(t)$  their norms.

In practice,  $t$  is a discrete variable since the signals are sampled. Therefore, the average angle  $\langle\theta\rangle$  is estimated as follows:

$$\langle\theta\rangle = \frac{1}{n} \sum_{t=1}^n \theta(t) \quad (2)$$

where  $n$  is the number of time samples in the observed cardiac cycle.

The second feature characterizes the similarity among the curves in terms of norms of the velocity vectors and is defined as follows:

$$C = \frac{\sum_{t=1}^n (N_1(t) - \bar{N}_1) (N_2(t) - \bar{N}_2)}{\sqrt{\sum_{t=1}^n (N_1(t) - \bar{N}_1)^2} \sqrt{\sum_{t=1}^n (N_2(t) - \bar{N}_2)^2}} \quad (3)$$

where  $\bar{N}_1$  and  $\bar{N}_2$  are the mean values of  $N_1$  and  $N_2$ , respectively.

Two SPOT curves that are homothetic, i.e., that are such that  $N_1(t) = \lambda N_2(t) \forall t$ , result in a value of  $C$  equal to 1.

To illustrate this, Table I gives the values of these two features resulting from the comparison between the arrhythmia SPOT curves of Fig. 2 and the NSR template.

### III. VT/SVT DISCRIMINATION BASED ON SPOT COMPARISONS

#### A. Overview of the Algorithm

As mentioned earlier, the method aims at comparing an arrhythmia beat with an NSR beat used as a reference (see Fig. 3). This reference template is obtained by averaging several consecutive normal beats during a slow heart rate episode in order to filter out beat-to-beat variations.

An arrhythmia is detected when the heart rate is above a predetermined threshold, typically higher than 100 beats per minute (BPM). In this case, morphological analysis is performed

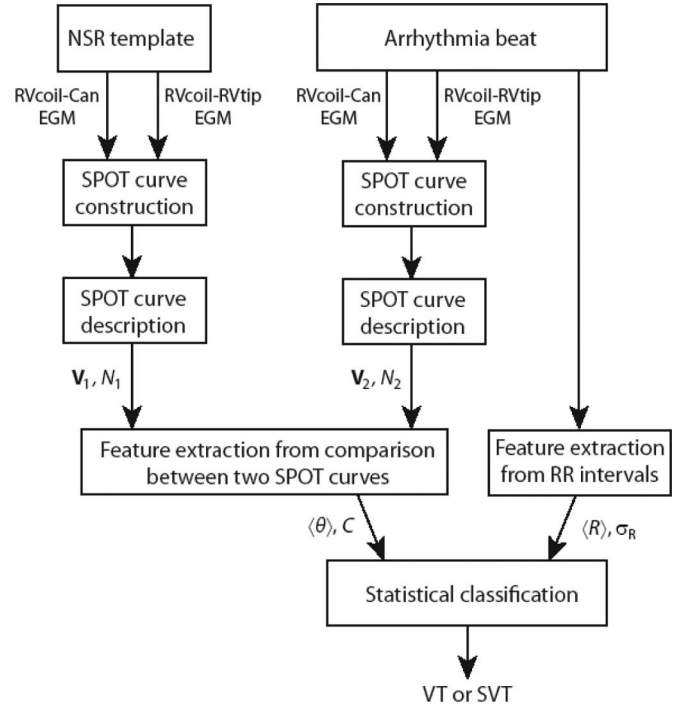


Fig. 3. Overview of the discrimination algorithm.

by computing the velocity vectors of the arrhythmia SPOT, and the morphological features  $\langle\theta\rangle$  and  $C$  between the arrhythmia SPOT and the reference template are estimated.

In addition to  $\langle\theta\rangle$  and  $C$ , two usual rhythmological features are taken into account: the mean value of RR intervals of the arrhythmia  $\langle R\rangle$  and the associated standard deviation  $\sigma_R$ . Actually, as illustrated by previous clinical trials ([4] and [10]), morphology algorithms perform better when combined with rhythm discriminators.

#### B. Support Vector Machines

The decision whether the arrhythmia is a VT or an SVT is then performed in the 4-D space spanned by  $\langle\theta\rangle$ ,  $C$ ,  $\langle R\rangle$ , and  $\sigma_R$ . For a given beat  $B$ , the first two features pertain to the  $(B, \text{NSR template})$  pair, and the last two to the arrhythmia episode containing  $B$ . The statistical classifier used at this point is a support vector machine (SVM) [11]; its purpose is to divide the 4-D space into two areas pertaining to VTs and SVTs, respectively.

A linear SVM classifier provides the optimal separating hyperplane in feature space, i.e., the separating hyperplane that classifies all examples without error, while at the same time, lying as far as possible from the closest examples. The distance between the separating hyperplane and the examples closest to it is called the *geometrical margin* of the classifier; the examples that lie at a distance from the separating hyperplane equal to the geometrical margin are called the *support vectors*. Denoting by  $\mathbf{X}$  the feature vector that describes the items to be classified (in our case, arrhythmia beats), and by  $\mathbf{W}$  the vector of parameters

of the model, the equation of the hyperplane is of the form

$$\mathbf{W} \cdot \mathbf{X} + b = 0 \quad (4)$$

where  $b$  is an additional parameter.

In our case, the components of the vector  $\mathbf{X}$  describing a beat are the aforementioned four features  $\langle \theta \rangle$ ,  $C$ ,  $\langle R \rangle$ , and  $\sigma_R$ .

*Training* is the procedure whereby the values of  $\mathbf{W}$  and  $b$  are estimated from the examples, i.e., from a data set (“training set”) containing heartbeat recordings that were labeled by experts with label  $+1$  for VT beats and  $-1$  for SVT beats. Training is cast in the form of a constrained optimization problem, where the function to be minimized is the norm of the vector of parameters  $\mathbf{W}$  under the constraint that all examples be correctly classified (“hard-margin” SVMs).

The central problem in machine learning is the ability of the trained models to generalize, i.e., to correctly classify examples that are not present in the training set. The fact that the magnitude of the vector of parameters is kept as small as possible minimizes the risk of poor generalization. However, allowing some examples of the training set to be misclassified may further improve the generalization ability of the model. This leads to “soft-margin SVMs,” where the function to be minimized contains, in addition to the norm of vector  $\mathbf{W}$ , a term that is roughly proportional to the number of misclassified examples, with a proportionality coefficient  $\gamma$  (termed the “regularization constant”), which must be determined in designing the model.

In this study, however, a more complex, nonlinear classifier is required. To this end, we apply the so-called “kernel trick” which maps the original observations (which are not linearly separable) onto a higher-dimensional space, where they are linearly separable, and a linear classifier can be used; this makes a linear classification in the new space equivalent to nonlinear classification in the original space (provided the kernel and its hyperparameters are chosen appropriately, as described in the next section). As a result, the built-in regularization mechanism inherent to linear SVMs, leading to the estimation of the parameters of the optimal separating hyperplane, is retained, while optimal nonlinear separating surfaces are estimated.

We use here a standard Gaussian radial basis kernel. In this case, the discriminant function obtained after training is given by

$$E(\mathbf{X}) = \sum_{i=1}^l \alpha_i \exp\left(\frac{-\|\mathbf{X} - \mathbf{X}_i\|^2}{2\sigma^2}\right) + b \quad (5)$$

where  $l$  is the number of support vectors,  $\mathbf{X}_i$  is the feature vector describing support vector  $i$ ,  $\mathbf{X}$  is the feature vector of a heartbeat to be classified,  $\alpha_i$  and  $b$  are parameters estimated during training, and  $\sigma$  is a “hyperparameter” chosen during model selection, as described in the next section.

If the decision threshold is set to 0, the equation of the separating surface is  $E(\mathbf{X}) = 0$ ; a heartbeat described by  $\mathbf{X}$  is classified as a VT beat if  $E(\mathbf{X}) > 0$ , otherwise it is classified as an SVT beat.

TABLE II  
DATABASES USED FOR CLASSIFIER TRAINING AND TESTING

Database name	# pts <sup>a</sup>	Gender (male)	Age	# SVTs	SVT BPM	# VTs	VT BPM
Sorin CRM	32	84%	56±19	19	100-160	29	110-370
AAEL I	41	83%	62±12	7	100-220	64	130-350
AAEL II	40	83%	61±13	7	100-170	90	110-360
ICD Data	10	60%	64±17	78	100-160	7	250-350

<sup>a</sup> # pts= number of patients.

### C. Model Selection

The effectiveness of SVM classification is contingent on the proper selection of the kernel hyperparameter  $\sigma$  and the soft margin hyperparameter  $\gamma$  (which controls the tradeoff between errors of the SVM on training data and margin maximization). In this study, model selection was performed using leave-one-out (LOO) cross validation [12], i.e., each of the  $N$  examples of the training set was used as a validation example, which was classified by a classifier trained on the other  $N - 1$  examples. Thus,  $N$  classifiers with the same values of  $\sigma$  and  $\gamma$  were trained, each of which classified the example that was left out during its training. For a given  $\{\sigma, \gamma\}$  pair, the numbers of true negatives, true positives, false negatives, and false positives among the left-out examples were then computed so that the sensitivity and specificity pertaining to the  $\{\sigma, \gamma\}$  pair could be derived. Finally, the LOO score  $S$  pertaining to the  $\{\sigma, \gamma\}$  pair was defined as a weighted sum of the sensitivity and the specificity of the classifier

$$S = \rho \times \text{sensitivity} + \text{specificity}. \quad (6)$$

The weight  $\rho$  defines a tradeoff between these two values. Here, we chose  $\rho = 2$  in order to emphasize sensitivity: a misclassified SVT (false positive) is less risky than a misclassified VT (false negative), which could lead to a patient’s death.

The procedure was iterated for different values of  $\sigma$  and  $\gamma$  in a prescribed range:  $\sigma \in [0.1; 4]$  and  $\gamma \in [0.05; 100]$ , and the pair of values that yielded the highest value of  $S$  was retained.

As  $S$  is a discrete variable, several models were selected. Thus, an additional criterion was implemented: for each pair of  $\sigma$  and  $\gamma$ , for which we obtained the maximum LOO score, an SVM classifier was trained with the total amount of training data, then the decision threshold was varied in order to draw the receiver operating characteristic curve [13]. The classifier’s parameters are set to the values  $(\sigma, \gamma)$  for which the area under the curve (AUC) is largest.

## IV. TRAINING AND TEST DATABASES

EGMs from three different databases were used in this study to train and test the classifiers (see Table II).

### A. Sorin CRM Private Database for Classifier Training

The first dataset is private, supplied by Sorin CRM. It is composed of induced arrhythmias during an electrophysiology

procedure. This database features 29 VTs and 19 SVTs from 32 patients ( $56 \pm 19$  years, 84% men, 44% ischemic heart disease). In order to match the clinical database presented in the following, the records were downsampled to 125 Hz. Since this database is not publicly available, it was used to train the classifier.

### B. Standard Database for Classifier Testing

Two different test sets were used: the first one consists of volumes I and II of the standard Ann Arbor Electrogram Libraries [14], which include 154 VTs and 14 SVTs from 81 patients ( $62 \pm 13$  years, 83% men, 43% coronary artery disease). This is the only available database that contains both far-field and near-field EGMs. Unfortunately, most arrhythmias are induced, whereas spontaneous episodes would be preferable since they correspond to the events the algorithm will have to process. The records were also downsampled to 125 Hz.

### C. Clinical Database for Classifier Testing

The second database overcomes the previous drawback since it was recorded directly in ICDs. A data-acquisition procedure is underway within a clinical study including patients implanted with a Paradym dual-chamber ICD (Sorin CRM). The device is programmed after implantation to record the two EGMs needed to construct the SPOT curves during arrhythmia episodes. At the time of writing this paper, 24 patients were involved in 11 centers in Europe. To date, 10 patients contributed for a total of 7 VTs and 78 SVTs.

## V. ASSESSMENT PROCEDURE AND RESULTS

The efficiency of the proposed methodology was assessed in two different ways: a “static” approach and a “dynamic” approach. The static approach, being the simplest one, aimed at estimating the performances of the classifier to separate VT and SVT posterior to the arrhythmia. The dynamic validation evaluated the performance in an online-like procedure, in which a decision must be made continuously throughout the arrhythmia episode.

### A. Static Approach

In this approach, an arrhythmia episode is viewed as a single point in the 4-D feature space:  $\langle \theta \rangle$  and  $C$  are estimated for each beat, and the mean value over the whole arrhythmia episode is computed. To minimize the effect of outliers on the mean, 10% of the values that are furthest away from the mean are discarded, before recomputing the mean. The two rhythmological features  $\langle R \rangle$  and  $\sigma_R$  are also computed over the entire arrhythmia.

Model selection was performed on the Sorin CRM database, as described in Section IV; it resulted in hyperparameter values of  $\sigma = 2.9$  and  $\gamma = 2$  with  $S = 2.301$  and  $AUC = 0.966$ .

The SVM classifier divided the feature space into two regions, providing the equation  $E(\mathbf{X}) = 0$  of the boundary surface, where  $\mathbf{X}$  is the 4-D feature vector. The value of  $\text{sgn}(E(\mathbf{X}))$  indicates the class of the arrhythmia described by vector  $\mathbf{X}$ .

TABLE III  
PERFORMANCE OF THE SVM CLASSIFIER

Approach	Database	Sensitivity % (FN) <sup>a</sup>	Specificity % (FP) <sup>a</sup>
Static	AAEL	98.7 (2)	85.7 (2)
Dynamic	AAEL	98.7 (2)	71.4 (4)
	ICD Data	100 (0)	94.9 (4)

<sup>a</sup> FN= False Negative, FP=False Positive.

Table III summarizes the results over the test set on the Ann Arbor Electrogram Libraries (AAEL) database. This “static” approach was not validated on the ICD database because many arrhythmias (SVTs) last for several hours and therefore cannot be represented by a single point in feature space: in this case, the “dynamic” approach is preferred.

### B. Dynamic Approach

Unlike the “static” approach for which we need the entire arrhythmia to make the decision, the “dynamic” assessment aimed at giving an online decision for VT/SVT discrimination. During an arrhythmia episode, each beat in turn was analyzed individually: the values of  $\langle \theta \rangle$  and  $C$  were computed for each beat from its SPOT curve. The other two features ( $\langle R \rangle$  and  $\sigma_R$ ) were estimated on an eight-beat-long sliding window ending with the current beat. Thus, each beat of the arrhythmia corresponds to one point in the 4-D feature space. The final decision is made according to the following rules.

- 1) If six out of eight consecutive beats are classified as VT, a “majority index” was set to VT.
- 2) If six out of eight consecutive beats are classified as SVT, the majority index was set to SVT.
- 3) Otherwise, the majority index was set to “no majority.”
- 4) If VT majority persists during 12 cycles, the arrhythmia is classified as a life-threatening arrhythmia and a therapy should be delivered.

The results of the dynamic approach are shown in Table III over the two test sets. The sensitivity on the AAEL database is not affected by the dynamic approach. However, we observe a loss in specificity: in the dynamic approach, one decision is made for each arrhythmia beat; therefore, for long duration SVT, the persistence could be reached once and the arrhythmia episode would be misclassified as a VT. In the static approach, such a short temporary change in morphology would have a negligible impact on the mean morphology of a long SVT episode. The notable result is the fact that no VT from the present ICD data would be misclassified. For the test set (AAEL + ICD data), we obtained a mean sensitivity of 98.8% and a mean specificity of 91.3%.

## VI. DISCUSSION

Two major issues need to be addressed for direct implementation into ICDs. First, we need to take into account the current computational capabilities of ICDs, and second, the accuracy of the algorithm relying on the comparison with the NSR template; the latter has to be chosen properly.

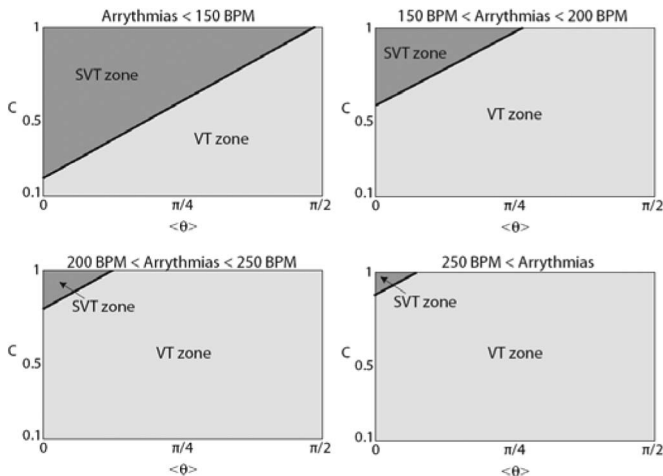


Fig. 4. Simplified boundary surfaces based on arrhythmia cardiac frequency.

### A. Simplified Approach Implemented in the ICD

Power consumption is a prominent issue in ICDs and the computational capabilities of the embedded processor are limited. In its original form, the algorithm described earlier is too demanding for implementation in the ICD. Therefore, a simplified version is proposed.

Furthermore, the computation of rhythmological features (stability, frequency, and sudden onset) has been carefully optimized for present-day processors. Therefore, the short-term future role of morphological algorithms should be to provide additional discrimination criteria, not to replace these existing features.

For these reasons, our efforts focused on simplifying the equation of the boundary surface and on decreasing the dimensionality of the feature space.

Plotting the 2-D level sets of  $E[\langle \theta \rangle C \langle R \rangle \sigma_R] = 0$  for fixed pairs of  $\langle R \rangle$  and  $\sigma_R$ , we observed that the cardiac frequency divided quite well the space in different zones: the higher the cardiac frequency, the smallest the SVT zone. We decided to cluster the arrhythmias into four groups: arrhythmias slower than 150 BPM, between 150 and 200 BPM, between 200 and 250 BPM, and above 250 BPM. The class boundaries are almost linear. Hence, they can be approximated by an affine function that is used to separate the VTs from the SVTs. The four zones are schematically represented in Fig. 4. In practice, arrhythmias faster than 250 BPM would be treated irrespective of the decision made by the classifier.

A second issue for the ICD onboard computation is the inverse cosine function needed for the computation of  $\langle \theta \rangle$ . It is less expensive to use  $\cos(\theta(t))$ . From equation (1), it is given by

$$\cos(\theta(t)) = \frac{b'_1(t)b'_2(t) + u'_1(t)u'_2(t)}{N_1(t)N_2(t)}. \quad (7)$$

The cosine function in  $[0, \pi]$  is a bijective function from  $[0, \pi]$  to  $[1, -1]$ . In order to compute a significant mean, we use  $T(t) = |\cos(\theta(t)) - 1|$ . Hence  $T(t)$  will be in  $[0, 2]$  and will vary in the same manner as the angle:  $T(t) = 0$  if  $\theta(t) = 0$ .  $\langle T \rangle$  spans  $[0, 2]$  instead of  $[0, \pi]$ . A new SVM classifier has been trained

TABLE IV  
PERFORMANCE OF THE SIMPLIFIED CLASSIFIER

Approach	Database	Sensitivity % (FN) <sup>a</sup>	Specificity % (FP) <sup>a</sup>
Dynamic	AAEL	96.8 (5)	100 (0)
	ICD Data	100 (0)	93.6 (5)

<sup>a</sup>FN= False Negative, FP=False Positive.

on the Sorin CRM database, projected on the aforementioned 2-D space, and evaluated on the test databases (see Table IV).

The performance is essentially the same; a small loss in sensitivity is observed, but a sizable improvement in specificity is obtained for induced arrhythmias (AAEL). Conversely, the performance of this new classifier on ICD data is almost identical to that reported in Table III.

### B. Template Updating

Template updating is a very important issue; EGM morphology may vary due to antiarrhythmic drugs, lead maturation, posture [7], disease progression [15], or ventricular cycle length [16].

The posture invariance of our representation was investigated. Recordings of NSR were performed for 24 patients in different body positions (sitting, standing, supine, prone, and left/right lateral decubitus). For 13 patients, the same recordings were performed a few months later, at the next followup. Recordings from a third followup are also available for two patients.

Based on the values of  $\langle \theta \rangle$  and  $C$  resulting from pairwise comparisons of templates at different postures, no significant changes in the SPOT features with respect to body position were observed. Moreover, as expected, a periodic update of the NSR template is necessary, especially during the first few months after implantation, where NSR changes are more important. For the moment, reestimation on a daily basis seems to be sufficient [17].

## VII. CONCLUSION

The SPOT-based morphological algorithm has allowed us to obtain very promising results on arrhythmia discrimination. Data acquisition is still underway, and our classifier will be tested on each new arrhythmia. A prospective clinical evaluation of an embedded version of the algorithm is being planned in order to confirm the advantages of this new analysis.

## ACKNOWLEDGMENT

The authors would like to thank Dr. E. Aimé (Istituto Di Ricovero e Cura a Carattere Scientifico (IRCCS) Policlinico San Donato, S. Donato M.se, Italy), and D. Contardi (SORIN Group Italia S.r.l., Milan, Italy), for their valuable help in collection of data from ICD recipient patients.

## REFERENCES

- [1] J. P. Daubert, W. Zareba, D. S. Cannom, S. McNitt, S. Z. Rosero, P. Wang, C. Schuger, J. S. Steinberg, S. L. Higgins, D. J. Wilber, H. Klein, M. L. Andrews, W. J. Hall, and A. J. Moss, "Inappropriate implantable cardioverter-defibrillator shocks in MADIT II: Frequency, mechanisms, predictors, and survival impact," *J. Amer. Coll. Cardiol.*, vol. 51, pp. 1357–65, Apr. 2008.

- [2] C. D. Swerdlow, M. L. Brown, K. Lurie, J. Zhang, N. M. Wood, W. H. Olson, and J. M. Gillberg, "Discrimination of ventricular tachycardia from supraventricular tachycardia by a downloaded wavelet-transform morphology algorithm: A paradigm for development of implantable cardioverter defibrillator detection algorithms," *J. Cardiovasc. Electrophysiol.*, vol. 13, pp. 432–441, May 2002.
- [3] M. R. Gold, S. R. Shorofsky, J. A. Thompson, J. Kim, M. Schwartz, J. Bocek, E. G. Lovett, W. Hsu, M. M. Morris, and D. J. Lang, "Advanced rhythm discrimination for implantable cardioverter defibrillators using electrogram vector timing and correlation," *J. Cardiovasc. Electrophysiol.*, vol. 13, pp. 1092–1097, Nov. 2002.
- [4] G. Boriani, M. Biffi, L. Frabetti, J. J. Lattuca, and A. Branzi, "Clinical evaluation of morphology discrimination: An algorithm for rhythm discrimination in cardioverter defibrillators," *Pacing Clin. Electrophysiol.*, vol. 24, pp. 994–1001, Jun. 2001.
- [5] G. Boriani, E. Occhetta, G. Pistis, C. Menozzi, M. Jorfida, S. Sermasi, M. Pagani, G. Gasparini, G. Musso, A. Dall'acqua, M. Biffi, and A. Branzi, "Combined use of morphology discrimination, sudden onset, and stability as discriminating algorithms in single chamber cardioverter defibrillators," *Pacing Clin. Electrophysiol.*, vol. 25, pp. 1357–1366, Sep. 2002.
- [6] L. Luthje, D. Vollmann, M. Rosenfeld, and C. Unterberg-Buchwald, "Electrogram configuration and detection of supraventricular tachycardias by a morphology discrimination algorithm in single chamber ICDs," *Pacing Clin. Electrophysiol.*, vol. 28, pp. 555–560, Jun. 2005.
- [7] T. Wolber, C. Binggeli, J. Holzmeister, C. Brunckhorst, U. Strobel, C. Boes, R. Moser, D. Becker, and F. Duru, "Wavelet-based tachycardia discrimination in ICDs: Impact of posture and electrogram configuration," *Pacing Clin. Electrophysiol.*, vol. 29, pp. 1255–1260, Nov. 2006.
- [8] M. Kotas, "Projective filtering of time-aligned ECG beats," *IEEE Trans. Biomed. Eng.*, vol. 51, no. 7, pp. 1129–1139, Jul. 2004.
- [9] P. Bouchet, R. Dubois, C. Henry, P. Roussel, and G. Dreyfus, "Spatial projection of tachycardia electrograms for morphology discrimination in implantable cardioverter defibrillators," *IEEE Proc. Comput. Cardiology*, vol. 36, pp. 9–12, Sep. 2009.
- [10] D. A. Theuns, M. Rivero-Ayerza, D. M. Goedhart, R. Van Der Perk, and L. J. Jordaens, "Evaluation of morphology discrimination for ventricular tachycardia diagnosis in implantable cardioverter-defibrillators," *Heart Rhythm*, vol. 3, pp. 1332–1338, Nov. 2006.
- [11] V. Vapnik, *The Nature of Statistical Learning Theory*. New York: Springer, 1995.
- [12] M. Stone, "Cross-validated choice and assessment of statistical predictions," (1974). *J. Roy Statist. Soc. B*, vol. 36, pp. 111–147, 1974.
- [13] X. H. Zhou, N. A. Obuchowski, and D. K. McClish, *Statistical Methods in Diagnostic Medicine*. New York: Wiley, 2002.
- [14] *Ann Arbor Electrogram Libraries*. Chicago, IL. Available: <http://www.electrogram.com>
- [15] S. J. Compton, J. J. Merrill, P. Dorian, J. Cao, D. Zhou, and J. M. Gillberg, "Continuous template collection and updating for electrogram morphology discrimination in implantable cardioverter defibrillators," in *Pacing Clin. Electrophysiol.* vol. 29, Mar. 2006, pp. 244–254.
- [16] D. A. Theuns, M. Rivero-Ayerza, D. M. Goedhart, M. Miltenburg, and L. J. Jordaens, "Morphology discrimination in implantable cardioverter-defibrillators: consistency of template match percentage during atrial tachyarrhythmias at different heart rates," *Europace*, vol. 10, pp. 1060–1066, Sep. 2008.
- [17] P. Milpied, R. Dubois, P. Roussel, C. Henry, and G. Dreyfus, "Stability of bipolar and unipolar endocardial electrograms," *IEEE Proc. Comput. Cardiology*, vol. 37, pp. 733–736, 2010.



**Paola Milpied** received the M.Sc. degree in bioinformatics and biostatistics from Université Paris-Sud XI, Paris, France, in 2007. She is currently working toward the Ph.D. degree at the Signal and Machine Learning (SIGMA) Laboratory, École Supérieure de Physique et de Chimie Industrielles (ESPCI) ParisTech, Paris, France.

Since 2008, she has been a Clinical Engineer with Sorin CRM, Clamart, France. Her current research interests include machine-learning-based embedded algorithms for implantable defibrillators.



**Rémi Dubois** (M'08) received the Ph.D. degree from Université Pierre et Marie Curie, Paris, France, in 2004. His Ph.D. thesis focused on machine learning approach to the early detection of heart diseases.

Since 2004, he has been an Associate Professor in the Signal and Machine Learning (SIGMA) Laboratory, École Supérieure de Physique et de Chimie Industrielles (ESPCI) ParisTech, Paris. His current research interests include machine learning techniques and advanced signal processing for medical applications.



**Pierre Roussel** received the Ph.D. degree in physics from the Université Pierre et Marie Curie, Paris, France, in 1991.

Since 1982, he has been an Associate Professor of Electronics and Automatic Control at École Supérieure de Physique et de Chimie Industrielles (ESPCI) ParisTech, Paris, France. His current research interests include the application of machine learning to various fields, classification on medical and biological applications, and dynamic modeling on natural phenomena.



**Christine Henry** received the M.Sc. degree in biomedical engineering from Université Paris XII, Créteil, France, in 1988.

She has held several positions in clinical research, mainly in the cardiac rhythm management area, for different companies. She is currently a Clinical Manager with Advanced Research, Sorin CRM, Clamart, France.



**Gérard Dreyfus** (M'83–SM'90) received the Ph.D. degree in physics from the Université Pierre et Marie Curie, Paris, France, in 1976.

In 1982, he was a Professor of Electronics and Automatic Control at École Supérieure de Physique et de Chimie Industrielles (ESPCI) ParisTech, Paris, where he currently heads the Signal Processing and Machine Learning (SIGMA) Laboratory. He has authored or coauthored 5 books, more than 200 publications in international journals or conferences, and 50 patents.

His current research interests include various aspects of machine learning (classification, static, and dynamic modeling), with special emphasis on its applications in computer-aided drug design, computer-aided diagnosis and therapy, and the dynamic modeling of complex natural systems.

Prof. Dreyfus is a member of the European Neural Network Society. He was an Associate Editor of the IEEE TRANSACTIONS ON NEURAL NETWORKS. He founded the French Chapter of the IEEE Computational Intelligence Society. He is a member of the IEEE Neural Network Technical Committee and of the IEEE Machine Learning for Signal Processing Committee.